GEOPHYSICAL RESEARCH LETTERS, VOL. 35, L05807, doi:10.1029/2007GL031791, 2008

Seeking sprite-induced signatures in remotely sensed middle atmosphere NO_2

E. Arnone,[1,2] A. Kero,[3] B. M. Dinelli,[4] C.-F. Enell,[3] N. F. Arnold,[5] E. Papandrea,[1] Craig J. Rodger,[6] M. Carlotti,[1] M. Ridolfi,[1] and E. Turunen[3]

Received 23 August 2007; revised 9 January 2008; accepted 30 January 2008; published 7 March 2008.

[1] The local chemical impact of sprites is investigated for the first time. This study is motivated by the current understanding of the streamer nature of sprites: streamers are known to produce NO_x, thus sprites are expected to lead to a local enhancement of the background abundances, and possibly impact ozone. We adopted the following strategy: middle atmosphere MIPAS/GMTR NO_2 satellite measurements were correlated with ground-based WWLLN detections of large tropospheric thunderstorms as a proxy for sprite activity. We found no evidence of any significant impact at a global scale, but an indication of a possible sprite induced NO_2 enhancement of about 10% at 52 km height in correspondence with active thunderstorms. This local enhancement appears to increase with height from a few percent at 47 km to tens of percent at 60 km.

Citation: Arnone, E., A. Kero, B. M. Dinelli, C.-F. Enell, N. F. Arnold, E. Papandrea, C. J. Rodger, M. Carlotti, M. Ridolfi, and E. Turunen (2008), Seeking sprite-induced signatures in remotely sensed middle atmosphere NO_2, *Geophys. Res. Lett.*, *35*, L05807, doi:10.1029/2007GL031791.

1. Introduction

[2] *Wilson* [1925] predicted that electrical discharges commonly observed in the troposphere could also occur tens of kilometers above thunderstorms. Only in 1989, middle atmosphere discharges, or transient luminous events (TLEs), were first accidentally observed with a video camera [*Franz et al.*, 1990], stimulating more than two decades of very intense research [e.g., *Neubert*, 2003; *Füllekrug et al.*, 2006]. Among the TLE family are red sprites, huge discharges extending from 40 to 90 km height, tens of kilometers wide and lasting a few tens of millisecond at most. Sprites are associated with intense thunderstorm activity, and are mainly produced by quasi electrostatic Joule heating induced by positive cloud to ground (+CG) lightning discharges [*Pasko et al.*, 1997]. Close-up images and high speed video recording [see, e.g., *Cummer et al.*, 2006] show sprites are typically initiated at about 75 km and develop upwards as a diffuse halo and downwards as streamers.

[3] Because of the similarity with other ionizing processes (e.g., aurorae or tropospheric lightning), it has been suggested that sprites may produce reactive NO_x and odd HO_x, thus possibly impacting ozone. The persistence of optical features and occasional reactivation of sprites support the possibility of an impact on the background chemistry [*Stenbaek-Nielsen et al.*, 2000]. However, due to major difficulties in detailed modeling and in direct observations of sprite chemical changes, to date no estimate of the chemical impact of sprites has been published.

[4] The major constraints in the observational study of sprite chemistry are the height of the events and the limited samples available. At a global rate of about 3 sprites per minute [*Ignaccolo et al.*, 2006], the likelihood of a coincidence between sprites and available satellite middle atmosphere spectroscopic measurements is very small. Moreover, reference observations of sprites are from nighttime optical images obtained during field campaigns [e.g., *Arnone et al.*, 2008] of limited extent in time and space. The usability of electromagnetic measurements [e.g., *Rodger*, 2003] or infrasound signatures [*Farges et al.*, 2005] associated with sprites is as yet uncertain. The best proxy for sprite activity is thus the causative tropospheric +CGs which are globally detected.

[5] In this paper we present the results of the first attempt to observe chemical changes induced by sprites.

2. Data and Methodology

[6] We used NO_2 measurements from the Michelson Interferometer for Passive Atmospheric Sounding (MIPAS) [*Fischer et al.*, 2007] instrument on board ESA ENVIronmental SATellite (ENVISAT). MIPAS is a limb-scanning Fourier Transform spectrometer recording emission spectra in the mid-infrared, 680 to 2410 cm^{-1}, with spectral resolution of 0.035 cm^{-1} FWHM, unapodized. Global coverage is assured by 14.3 daily orbits, each with observations at about 10.00 am and 10.00 pm local time. In the adopted standard mode, one orbit consists of 72 limb-scans, each recording 17 observations at tangent altitudes between 6 and 68 km. MIPAS instantaneous field of view (IFOV) is 3 km in height and 30 km in longitude. In latitude, i.e. along the line of sight crossing the atmosphere below 80 km, the IFOV footprint is about 1200 km at 52 km height, and 500 km at 60 km height. NO_2 was retrieved adopting the new Geo-fit Multi-Target Retrieval (GMTR) algorithm [*Carlotti et al.*, 2006]. Unlike common single profile methods, GMTR performs a 2-dimensional retrieval of a whole orbit that makes it possible to model the horizontal

[1]Dipartimento di Chimica Fisica e Inorganica, Università di Bologna, Bologne, Italy.
[2]Formerly at Department of Physics and Astronomy, University of Leicester, Leicester, U.K.
[3]Sodankylä Geophysical Observatory, University of Oulu, Sodankylä Finland.
[4]Istituto di Scienza dell'Atmosfera e del Clima, CNR, Bologne, Italy.
[5]Department of Physics and Astronomy, University of Leicester, Leicester, U.K.
[6]Department of Physics, University of Otago, Dunedin, New Zealand.

0094-8276/08/2007GL031791$05.00

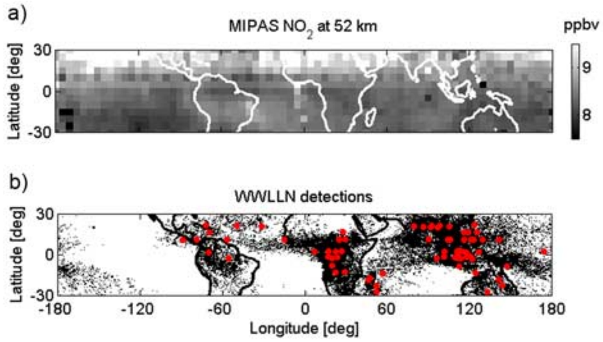

Figure 1. (a) Mean nighttime NO_2 at 52 km height by MIPAS and (b) WWLLN lightning activity (black, detections between 21 and 22 local hour; red, WWLLN-MIPAS coincidences) for the period August to December 2003.

inhomogeneity of the atmosphere. NO_2 was retrieved at the end of the cascade of all retrieval main targets, following a multi-target retrieval for p, T, H_2O and ozone. The random errors are about 0.5 ppbV (about 5%) in volume mixing ratio (VMR) at 52 km, which is a factor 2 to 4 lower than standard retrievals.

[7] We used lightning data as a proxy of sprite activity, reported by the World Wide Lightning Location Network (WWLLN) [*Rodger et al.*, 2006]. The network exploits the electromagnetic power radiated into the very low frequency radio band (3–30 kHz) by strong lightning discharges. WWLLN detects only a few percent of the world's lightning strokes, corresponding to those with the largest peak currents. Even though a direct correlation with sprites would require information about the polarity and the charge moment of the lightning discharge, the proxy adopted identify the regions with the highest likelihood of sprite activity. In fact, WWLLN has been shown to detect nearly all lightning producing storms [*Jacobson et al.*, 2006]. For the time period of our MIPAS-WWLLN comparison, WWLLN consisted of 11 stations, with a global detection efficiency of 1% which was strongly biased towards the Maritime Continent and away from the strong chimney regions in central Africa and the Americas.

[8] NO_2 was studied in the period August to December 2003, when both MIPAS/GMTR and WWLLN data were available. We used nighttime measurements of NO_2 because of the long persistence of possible sprite perturbations in the absence of photochemistry. Moreover, at night NO is promptly converted into NO_2, so that nighttime NO_2 is an excellent proxy for NO_x. The correlation between MIPAS measurements and intense lightning activity was obtained by integrating the number of WWLLN lightning strokes recorded within a coincidence window. The window was shaped according to the MIPAS IFOV footprint and located around the geolocation of the NO_2 measurement; for consistency, we adopted a 30 km $\times$ 500 km IFOV footprint for all heights. The period included in the integration was up to 60 minutes prior to the NO_2 observation. An NO_2 measurement was considered in coincidence with intense lightning activity (and thus high likelihood of sprite activity) if the integrated WWLLN lightning strokes number passed a threshold of 10 events per coincidence window. We call these NO_2 measurements WWLLN-NO_2 to distinguish them from background NO_2 (i.e. all available night NO_2 measurements).

[9] We considered NO_2 measurements over narrow latitude bands of 5° (MIPAS meridional resolution) to avoid including latitudinal changes. We detrended all available measurements within the selected band using a 100-points (100 satellite passes, about one week) running mean, and studied the NO_2 anomalies (i.e. difference to the running mean). The threshold of 10 lightning strokes was the best choice to minimize spurious correlations when considering individual latitude bands. Once all bands were studied together, the signal to noise increased and we could lower the threshold to a less conservative 5 lightning strokes.

[10] We also considered a first order effect of transport due to horizontal winds: we performed a second analysis where the coincidence window was translated upwind along a linear backward trajectory obtained adopting zonal and meridional winds from ECMWF operational analysis [*Uppala et al.*, 2005]. We refer to this latter correlation as "dynamical" correlation, to distinguish it from the former "static" correlation.

3. Results and Discussion

[11] Sprites are typically observed over the tropics and mid latitudes where intense lightning activity occurs. However, during 2003, the mid latitudes were partly affected by the strong high latitude winter NO_2 variability induced by downward transport of thermospheric NO_x and solar proton events. We thus focused over the tropics to maximize our chances to identify possible sprite-induced signatures. Inspection of global NO_2 (see Figure 1a) showed no evidence of a correlation with high lightning activity, for example, over land or in correspondence of the overall WWLLN detections (Figure 1b, black). This suggests sprite perturbations have no significant impact at global scale (or give at most a zonally-smoothed contribution) and need to be analyzed at a local level.

3.1. NO_2 Anomalies Over a Narrow Latitude Band

[12] Figure 2 shows the results of the analysis performed for nighttime NO_2 at 52 km over the 5°N–10°N latitude band. This latitude band had the best combination of high number of MIPAS measurements and WWLLN coincidences. The 52 km height was chosen as best compromise between best quality of the measurement (at and below 52 km) and highest expected sprite impact (roughly above 50 km height). The time series of background NO_2 VMR (Figure 2a, black, 1542 measurements) show average absolute values of about 10 ppbV and a standard deviation about the running mean of 1.5 ppbV. Random errors on a single measurement are 0.5 ppbV. WWLLN-NO_2 (Figure 2a, red, 14 measurements) were calculated with a static coincidence window over a period of 60 minutes prior to MIPAS observations. The window was twice as wide (along longitude) as the MIPAS IFOV footprint to partly account for uncertainties and transport, and the lightning stroke threshold number was 10. This high lightning threshold implies that we are considering only thunderstorms with intense lightning activity, and thus high likelihood of sprite occurrence.

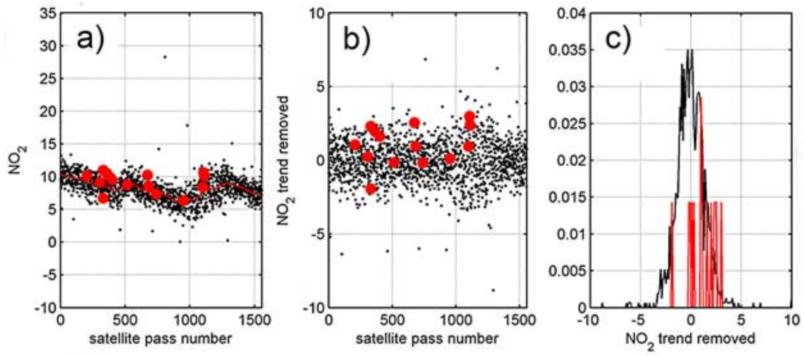

Figure 2. (a) MIPAS single measurements time series (black, nighttime background NO_2, red, nighttime NO_2 in coincidence with WWLLN lightning activity—WWLLN-NO_2) within the latitude band 5°N to 10°N and at 52 km height; (b) NO_2 anomalies time series (trend removed); and (c) distribution of NO_2 anomalies (the WWLLN-NO2 in red is scaled by a factor 0.2). See text for details.

[13] All WWLLN-NO_2 fall within the main range of background NO_2, thus suggesting a possible sprite impact no larger than background variability. However, the WWLLN-NO_2 shows a tendency to be above the trend (red line). We detrended the selected sample (Figure 2b) and analyzed the distribution of the anomalies about the running mean (Figure 2c). The WWLLN-NO_2 distribution shows a positive displacement of about +1 ppbV (about +10%) compared to the background NO_2. A bootstrap statistical analysis of the two distributions was performed showing that the risk of statistical coincidence is 1%. The difference is thus statistically significant.

[14] No vertical transport could bring about changes in middle atmosphere NO_2 within tens of minutes from enhanced tropospheric lightning activity. The NO_2 enhancement must thus be due to in situ production, or by retrieval artifacts. The former interpretation would require middle atmosphere processes associated with tropospheric lightning activity which current knowledge identifies as sprites. We discuss the latter unlikely possibility in Section 3.3.

[15] Repetition of the analysis over other latitude bands (see red dots in Figure 1b for the geolocation of all WWLLN-NO_2) showed a lack of consistency of the displacement: out of 4 latitude bands where we had an acceptable number ($\geq$10) of WWLLN-NO_2 coincidences, 2 showed a positive enhancement of +1 ppbV, one no change, and one a negative displacement of −0.4 ppbV. This lack of consistency is not unexpected since not all lightning is associated with sprite activity. On average a sprite may occur every 1000 lightning flashes [*Ignaccolo et al.*, 2006]: given that in 2003 WWLLN detected 1–2% of the world strongest lightning, and the threshold of 10 lighting strokes we imposed, one could expect one sprite every 2 WWLLN-NO_2 coincidences, further reduced by about a factor 2 accounting for geolocation uncertainties. However, rather than a one-to-one correlation, the selected WWLLN data should be interpreted as strong thunderstorm activity, implying high likelihood of sprite occurrence. Figure 1b confirms all WWLLN-NO_2 (red dots) are located over thunderstorm regions. To increase the numbers of our statistics, we analyzed the overall distribution of these anomalies over the tropics.

3.2. Overall Distribution of NO_2 Anomalies Over the Tropics

[16] The distributions of NO_2 anomalies over all individually detrended 5 degrees latitude bands in the range 30°S to 20°N was calculated. WWLLN-NO_2 were obtained integrating over time windows of 10, 20, 30 and 60 minutes prior to the MIPAS observation and using a threshold of 5 lightning strokes. Figure 3 shows the results of the overall distribution of NO_2 anomalies in the range 30°S to 20°N for the 20 minutes time window static correlation, at 60, 52 and 47 km height. In the 52 km case, the dynamical correlation distribution is also shown (Figure 3b, red).

[17] At 52 km height (Figure 3b), the overall static WWLLN-NO_2 distribution (gray line) shows an asymmetry compared to the background NO_2 (shaded). The displace-

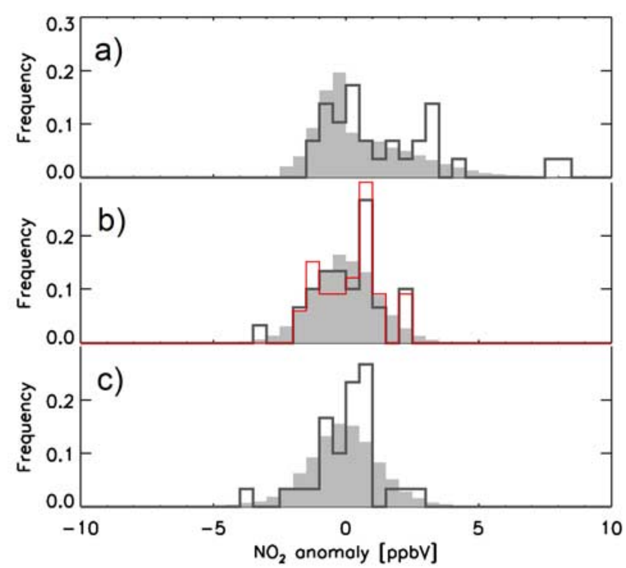

Figure 3. Global distribution of NO_2 anomalies over the region 30°S to 20°N (shaded, NO_2; gray line, WWLLN-NO_2), with static coincidence window of 20 minutes and 30 km × 500 km. Measurements are for heights (a) 60 km, (b) 52 km, and (c) 47 km. At 52 km height the dynamical correlation case is superimposed (red).

ment in the mean value observed in the 5°N–10°N case is not present any more (both the mean and the median are shifted by only +0.05 ppbV). Any possible sprite perturbation thus falls within the background variability. However, there is a pronounced peak at about +1 pbbV in the WWLLN-NO_2 distribution, which is in agreement with enhancements observed within the single narrow bands. The peak is at values larger than the random error of the retrieval (0.5 ppbV) so it is well resolved. This peak persists when increasing the time window to 30 minutes and fades at 60 minutes (not shown) when transport processes may become too important to be neglected.

[18] The dynamical case (Figure 3b, red line) takes into account a first order transport due to horizontal winds. We analyzed the lightning activity (proxy of sprite activity) at upwind locations from where NO_2 perturbations may have been transported to the location of the observation during the time-window. Because of the linear approximation adopted for the backward trajectories, one expects an improvement only over short time scales. Interestingly, we find that the dynamical WWLLN-NO_2 distribution increases its asymmetry with a more pronounced peak at +1 ppbV, differentiating more significantly from the background NO_2 distribution. The WWLLN-NO_2 anomaly distribution has now a mean of +0.2 ppbV and a median of +0.5 ppbV which confirms the change induced by considering sources of sprite activity at a more realistic geolocation. Increase of the time-window to 30 and 60 minutes (not shown) leads to weaker differences with the static case. However, the peak at +1 ppbV is still (just) visible in the 60 minutes dynamical case.

[19] These results suggest that a significant fraction of all WWLLN-NO_2 coincidences (possibly 15–20%) show an enhancement of about +1 ppbV compared to background NO_2, i.e. a +10% change. This fraction is roughly compatible with the expected number of coincidences deduced from the sprite to lightning occurrence ratio discussed above.

[20] At 47 km (Figure 3c) the distribution is more compact and symmetric, possibly because of the higher background NO_2 VMR absolute values. The WWLLN-NO_2 anomaly distribution shows a peak at about 0.5 ppbV, peak that decreases to a few tenths of ppbV at 42 km (not shown). At 60 km height (Figure 3a), the background NO_2 distribution loses compactness, and so does the WWLLN-NO_2 distribution. However, the WWLLN-NO_2 seems to show stronger NO_2 enhancements, which is confirmed by a median of +0.9 ppbV against a background median of −0.1 ppbV. The strongest enhancements reach +8 ppbV which is 8 times larger than the most common background values. At 68 km height the retrieved NO_2 is not meaningful. Part of the NO_2 anomalies in coincidence with lightning activity (and thus sprite activity) seems to be biased towards a range of higher NO_2 values. This increase of the NO_2 enhancement with height is compatible with an expected sprite signature: fewer sprite events extend below 50 km height compared to 60 km height and above.

3.3. Robustness of the Analysis

[21] To investigate the robustness of our results we performed a series of Monte Carlo tests. Firstly, a bootstrap simulation showed that the risk of coincidence of the background NO_2 and the WWLLN-NO_2 52 km distribution is about 5%. Secondly, in order to minimize the differences to the real case, we further produced *fake* lightning activity by shifting the dates of the real one, thus maintaining the original spatial and temporal characteristics. No physical correlation with NO_2 is possible with the fake data set. Repetition of the complete analysis for 100 fake distributions showed that positive peaks of similar magnitude could be randomly reproduced in about 30% of the cases. This is not unexpected since the peak falls within the background variability. However, only in 8 fake distributions, the 52 km peak increases its magnitude applying backward trajectories, and only in 1 fake case a consistency of the dynamical case and the static case at the three heights was found.

[22] We also performed a series of tests on the possible cloud contamination on our retrieval, and found that no change in the retrieved NO_2 occurs when clouds at various heights are considered. Independent radiative transfer simulations of the dependence of vertical profiles on the presence of clouds confirm that no change occurs above 20–25 km (H. Sembhi, personal communication, 2007), thus far below our retrieved NO_2 (42 to 68 km height).

4. Conclusions

[23] In order to find possible sprite-induced NO_x changes, we studied nighttime satellite measurement of NO_2 at 50–60 km height in coincidence of strong tropospheric lightning activity. We found no global impact, but a local enhancement in NO_2 is coincidence with intense lightning activity of about +10% at 52 km height visible as a well defined peak within the background variability. Consideration of transport processes leads to a better defined peak at the same magnitude of the enhancement, while the latter increases with increasing height, from a few percent at 47 km to tens of percent at 60 km. A Monte Carlo test showed this consistency could be found only in one out of 100 cases.

[24] Our analysis points towards a local sprite effect upon the composition of the neutral atmosphere, with a more robust evidence in the band 5–10N. These results are consistent with the ion-chemistry modeling estimates we present in a companion paper [*Enell et al.*, 2008]. However, due to the small numbers of our analysis and the small magnitude of the changes, an extension of the analysis to a larger data set is needed to confirm these results.

[25] **Acknowledgments.** E. Arnone and C.-F. Enell acknowledge funding through the European Community's Human Potential Programme under contract HPRN-CT-2002-00216, Coupling of Atmospheric Layers, during 2003–2006. E. A. acknowledges a travel grant from the Finnish Academy of Science and Letters, Vilho, Yrjö and Kalle Väisälä Foundation. ECMWF Operational Analysis are from the British Atmospheric Data Centre (http://badc.nerc.ac.uk/data/ecmwf-op/).

References

Arnone, E., et al. (2008), The Eurosprite 2005 campaign, in *Proceedings of the 33rd Annual European Meeting on Atmospheric Studies by Optical Methods*, *IRF Sci. Rep. 292*, edited by J. Arvelius, Swedish Inst. of Space Phys., Kiruna, in press.

Carlotti, M., G. Brizzi, E. Papandrea, M. Prevedelli, M. Ridolfi, B. M. Dinelli, and L. Magnani (2006), GMTR: Two-dimensional geo-fit multitarget retrieval model for Michelson Interferometer for Passive Atmospheric Sounding/Environmental Satellite observations, *Appl. Opt.*, *45*, 716–727.

Cummer, S. A., N. Jaugey, J. Li, W. A. Lyons, T. E. Nelson, and E. A. Gerken (2006), Submillisecond imaging of sprite development and structure, *Geophys. Res. Lett.*, *33*, L04104, doi:10.1029/2005GL024969.

Enell, C.-F., et al. (2008), Parameterisation of the chemical effect of sprites in the middle atmosphere, *Ann. Geophys.*, *26*, 13–27.

Farges, T., E. Blanc, A. Le Pichon, T. Neubert, and T. H. Allin (2005), Identification of infrasound produced by sprites during the Sprite2003 campaign, *Geophys. Res. Lett.*, *32*, L01813, doi:10.1029/2004GL021212.

Fischer, H., et al. (2007), MIPAS: An instrument for atmospheric and climate research, *Atmos. Chem. Phys. Discuss.*, *7*, 8795–8893.

Franz, R. C., R. J. Nemzek, and J. R. Winckler (1990), Television image of a large upward electrical discharge above a thunderstorm system, *Science*, *249*, 48–51.

Füllekrug, M., E. A. Mareev, and M. J. Rycroft (Eds.) (2006), *Sprites, Elves and Intense Lightning Discharges, NATO Sci. Ser. II*, vol. 225, Springer, New York.

Ignaccolo, M., T. Farges, A. Mika, T. H. Allin, O. Chanrion, E. Blanc, A. C. Fraser-Smith, and M. Füllekrug (2006), The planetary rate of sprite events, *Geophys. Res. Lett.*, *33*, L11808, doi:10.1029/2005GL025502.

Jacobson, A. R., R. Holzworth, J. Harlin, R. Dowden, and E. Lay (2006), Performance assessment of the World Wide Lightning Location Network (WWLLN), using the Los Alamos Sferic Array (LASA) as ground truth, *J. Atmos. Oceanic Tech.*, *23*, 1082–1092.

Neubert, T. (2003), On sprites and their exotic kin, *Science*, *300*, 747–749.

Pasko, V. P., U. S. Inan, T. F. Bell, and Y. N. Taranenko (1997), Sprites produced by quasi-electrostatic heating and ionization in the lower ionosphere, *J. Geophys. Res.*, *102*, 4529–4561.

Rodger, C. J. (2003), Subionospheric VLF perturbations associated with lightning discharges, *J. Atmos. Sol. Terr. Phys.*, *65*, 591–606.

Rodger, C. J., S. Werner, J. Brundell, E. Thomson, N. R. Lay, R. Holzworth, and R. Dowden (2006), Detection efficiency of the VLF World-Wide Lightning Location Network (WWLLN): Initial case study, *Annal. Geophys.*, *24*, 3197–3214.

Stenbaek-Nielsen, H. C., D. R. Moudry, E. M. Wescott, D. D. Sentman, and F. T. S. Sabbas (2000), Sprites and possible mesospheric effects, *Geophys. Res. Lett.*, *27*, 3829–3832.

Uppala, S., et al. (2005), The ERA-40 re-analysis, *Q. J. R. Meteorol. Soc.*, *131*, 2961–3012.

Wilson, C. T. R. (1925), The electric field of a thundercloud and some of its effects, *Proc. Phys. Soc. London*, *37*, 32D–37D.

N. F. Arnold, Department of Physics and Astronomy, University of Leicester, Leicester, LE1 7RH, U.K.

E. Arnone, M. Carlotti, E. Papandrea, and M. Ridolfi, Dipartimento di Chimica Fisica e Inorganica, Università di Bologna, I-40136 Bologna, Italy. (enrico.arnone@unibo.it)

B. M. Dinelli, Istituto di Scienza dell'Atmosfera e del Clima, CNR, I-40129 Bologna, Italy.

C.-F. Enell, A. Kero, and E. Turunen, Sodankylä Geophysical Observatory, University of Oulu, FI-99600 Sodankylä, Finland.

C. J. Rodger, Department of Physics, University of Otago, Dunedin, 9016, New Zealand.